International Journal of Science and Research (IJSR)
ISSN: 2319-7064
SJIF (2022): 7.942

Endoscopic Access Possibility in Maxillary Sinus Floor Augmentation

Desislava Stoyanova[1], Stefan Peev[2], Nikolay Sapundziev[3], Anjela Bakhova[4]

[1, 2]Department of Periodontology and Dental Implantology, Medical University of Varna, Bulgaria

[3]Department of Neurosurgery and Otorhinolaryngology, Medical University of Varna, Bulgaria

[4]Faculty of Public Health, Medical University of Varna, Bulgaria

Abstract: ***The purpose of this study is to determine the optimal endoscopic approach with the highest share of visibility (SV) from the maxillary sinus floor (MSF). Materials and methods: An experimental study was conductedwhere SV of the maxillary sinus total surface area was measured on twenty 3D simulation models by using a built-in optics endoscope with angular visual axis deflected from 15⁰ - 90⁰. Results. There was no statistically significant difference in the share of the total field of view of MSF compared to the medial, central and distal endoscopic access openings at endoscope penetration of 10 mm and endoscope viewing angle of 45°, p≥0.05. The SV of the total field of view of MSF was the same for all three openings, and this was the highest compared with all other observations performed. Conclusion: The highest SV from the total field of view of MSF was observed in all three endoscopic access openings (medial, central, distal) with the endoscope penetration at 10 mm and viewing angle at 45°. The lowest SV of the total field of view of MSFwas observed at the distal opening with an endoscope penetration of 20 mm and viewing angle of 15°.***

Keywords: endoscope, share of visibility, maxillary sinus floor, 3d models, endoscopically navigated surgery

1. Introduction

The history of paranasal sinuses diagnostic endoscopy started more than 120 years ago. In Berlin in 1901, A. Hirschmann performed the first maxillary sinus endoscopies using a modified cystoscope with a diameter of 5 mm, introducing it through the alveolus of a previously extracted tooth, and thus he was able to take the first pictures of chronic maxillary sinusitis. In 1903, he introduced the diagnostic function of the endoscope alone, which he also used to examine nose, ear, and epipharynx, describing it in his article "On Endoscopy of the Nose and Paranasal Sinuses" (6).

Medicine and dentistry development in recent years towards minimally invasive procedures has necessitated the increasing use of navigated endoscopic surgery (3).

Technological advancements in endoscopic rigid systems using integrated optics with an angular visual axis, deviated with respect to the instrument axis, improve visualization of the surgical field and contribute to more precise and atraumatic surgery (8).

Köhler et al. (6) concluded,that the endonasal approaches for the treatment of maxillary sinus disease described in otorhinolaryngology prove to be inapplicable to the needs of dental implantology and more specifically to the performance of endoscopic- guided MSF augmentation procedure, as they cannot provide an overview optical, atraumatic, and direct view of MSF above the Schneiderian membrane. The authors state, that an approach along the fossa canina called anthroscopy- time honored, but long overlooked, is appropriate for the needs of dental implantology when performing an endoscopically assisted MSF elevation procedure.

Engelke et al. has suggested special endoscopic techniques for the needs of dentistry that are comparable in many respects to the techniques used in otorhinolaryngology. They are direct endoscopy, immersion endoscopy, supported endoscopy, support immersion endoscopy, and trocar-guided endoscopy. Anthroscopy is performed in the canter of the canine fossa and requires puncture of the anterior wall of the maxillary sinus by a trocar. Shaping the opening to a diameter of 5 mm provides a space between MSF and Schneiderian's membrane and the endoscope, which is named subantral space. Anthroscopy is a procedure for direct endoscopic visualization for the purpose of biopsies, removal of foreign bodies, evaluation of the Schneiderian membrane in the cases of suspected inflammation, and detection and control of perforations of the Schneiderian membrane when it is elevated during an MSF augmentation procedure and control of the positioning of the barrier membrane and bone repair material during the MSF augmentation procedure (3).

2. Materials and Methods

An experimental study was conducted on maxilla and maxillary sinuses three-dimensional simulation models. For the development of these three-dimensional simulation models, 20 preoperative CBCT images of patients who underwent sinus floor augmentation procedures with lateral approach were selected. The selected preoperative CBCT images for the development of the three-dimensional models were of 10 male and 10 female patients.

Using the CBCT image processing software "Planmeca Romexis", an image was generated to output an STL file. The prepared STL files of the three-dimensional models were printed using 3Dfactories' "Visions3Dprinter". The principle of operation of this printer is FDM (Fused Deposition Modeling) - the model is built by additively

depositing a fused material (PLA - filament).The material is a filament with a diameter of 1.75 mm wound on a roll. The printer extruder has a diameter of 0.3 mm, the maximum printing speed is 80 mm/s. Ready STL files are prepared for printing by using "3Dfactories - Repetier - Host V1.0.6", and the same individual printing operating parameters are set for all 20 models to meet the needs of our task – model quality assurance - 0.08 mm (high quality), type of adhesion of the model to the table - Raft and maintenance of model by touching the table. The printing speed and the printing speed of the outer perimeter of the printed model is the same - 38 mm/s - slow type. The fill speed is 45 mm/s and the density is 60%. After completing the printing process, the 3D simulation models are subjected to cleaning of the support elements. The 3D simulation models are scaled 1:1 relative to the patients. In order to conduct the study of each 3D model in the antero-posterior direction, a millimetre paper was placed on each maxillary sinus floor, whose length was individualized according to the individual characteristics of each patient and its width is 5 mm (Figure 1).

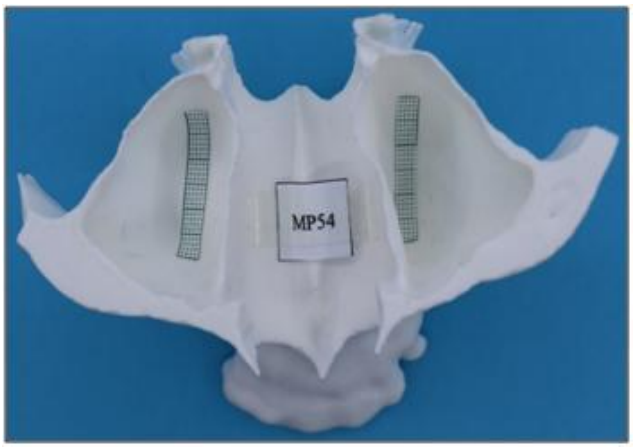

Figure 1

On each maxillary sinus anterior wall, three openings, medial, central and distal, were performed by using a 5 mm diameter trocar with a distance of 8 mm between the centres of the holes. To locate the centre of the medial opening, the projection of the canine tooth 5 mm in vertical direction and then 5 mm in distal direction is taken as starting point (Figure 2).

On each sinus of the 3D models, a visibility fraction measurement of the maxillary sinus total surface area in the antero-posterior direction was conducted using a Karl Storz ENDOCAMELEON ENT HOPKINS Telescope with built-in optics with the angled visual axis deflected from 15º - 90º to the instrument axis.

Figure 2

Measurement of SV of the maxillary sinus total surface area was performed with the visual axis deflected to 15º, 45º and 90º to the instrument axis. SV of the maxillary sinus total surface area is established by relating the individual maxillary sinus length to the observed instantaneous length at the different visual axes of the selected 15º, 45º and 90º (Figure 3, 4 and 5).

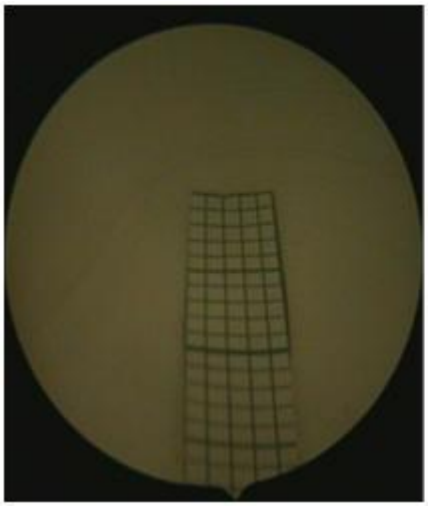

Figure 3

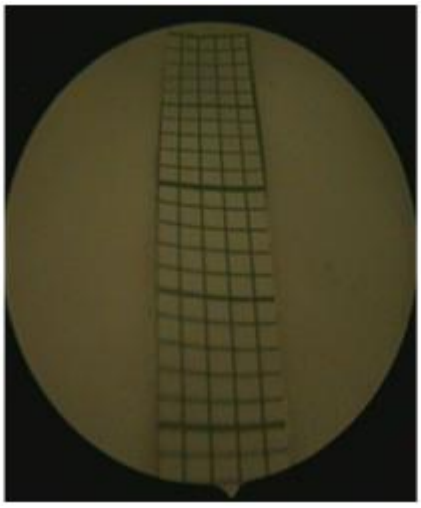

Figure 4

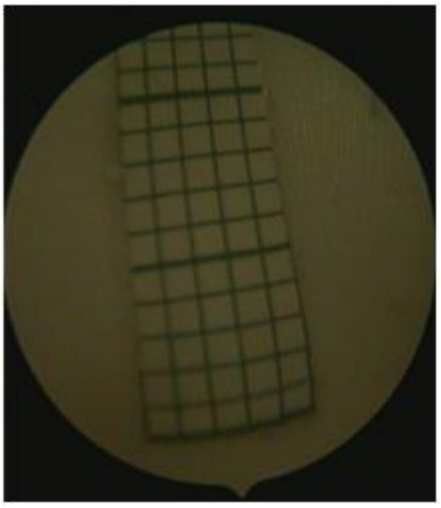

Figure 5

To measure SV of the MSF total area, the endoscope was advanced in the antero-posterior direction 10 mm and 20 mm into each performed medial, central and distal opening of each sinus, which was observed at visual axes 15º, 45º and 90º to the instrument axis and the lowest focal angle.

SV dataof MSF total surface area are visible in table 1. SV data of the maxillary sinus total surface area was analyzed against the endoscopic access opening, endoscope penetration depth, and endoscope viewing angle using IBM SPSS Statistics 25. The following statistical methods were

applied to perform the statistical analysis of the collected data: parametric tests - Student's t-test for dependent samples and ANOVA - test to compare more than two groups and non-parametric tests - Wilcoxon test for dependent samples, Kruskal -Wallis and Fridman test to compare more than two groups.

3. Results

It was found that the distribution of SV data of MSF total field of view for a medial opening with a penetration depth of 20 mm and endoscope viewing angle 90° and distal opening with 10 mm depth of penetration and 15° endoscope viewing angle was not normal, and the distribution of data for medial, central and distal opening with 10 and 20 mm depth of penetration and 15°, 45° and 90° endoscope viewing angle was normal.

Thirty-one observations were not included in the data analysis due to zero SV of MSF total observation area. This zero visibility was observed at the medial, central and distal openings with an endoscope penetration of 20 mm and a viewing angle with the endoscope of 15°. For medial are 9, for central - 8 and for distal - 14.

Data analysis to endoscopic access opening
The analysed data for SV of MSF total field of view to the endoscopic access opening are shown in table 2.

There was no statistically significant difference in SV of MSF total field of view relative to the medial, central, and distal endoscopic access openings at an endoscope penetration of 10 mm and an endoscope viewing angle of 45°, $p \geq 0.05$. SV of MSF total field of view was the same for all three openings, and this SV was the highest compared with all other observations performed.

From the data analysis, there was a statistically significant difference in SV of the total field of view MSF from the medial, central and distal openings at an endoscope penetration of 10 mm and an viewing angle with the endoscope of 15° - $p \leq 0.05$, with SV of the total field of view of MSF decreasing from the medial (0.07 ± 0.03) to the distal opening (0.04 ± 0.02). There was a statistically significant difference in the share of the total field of view of MSF to the medial, central, and distal openings at an endoscope penetration of 20 mm and an endoscope viewing angle of 15° - $p \leq 0.05$, with the share of the total field of view of MSF decreasing from the medial (0.04 ± 0.02) to the distal opening (0.02 ± 0.01). There was a statistically significant difference in the share of the total field of view of MSF to the medial, central, and distal openings at an endoscope penetration of 20 mm and an endoscope viewing angle of 45°, $p \leq 0.05$, with the share of the total field of view of MSF decreasing from the medial (0.08 ± 0.02) to the distal opening (0.07 ± 0.02). There was a statistically significant difference in the share of the total field of view of MSF to the medial, central, and distal openings at an endoscope penetration of 10 mm and an endoscope viewing angle of 90°, $p \leq 0.05$, with the share of the total field of view of MSF increasing from the medial (0.06 ± 0.02) to the distal opening (0.08 ± 0.02). There was a statistically significant difference in the share of the total field of view of MSF to the medial, central and distal openings at an endoscope penetration of 20 mm and an endoscope viewing angle of 90° - $p \leq 0.05$, with the share of the total field of view of MSF increasing from the medial (0.08 ± 0.02) to the distal opening (0.10 ± 0.02).

Data analysis to endoscope penetration depth
The analysed data for SV of total field of view of MSF to the depth of endoscope penetration are shown in table 3.

There was a statistically significant difference of SV of the total field of view of MSF in the medial opening at an endoscope viewing angle of 15° to endoscope penetration depth of 10 and 20 mm, respectively, $p \leq 0.05$, with SV of the total field of view of MSF decreasing from 10 (0.07 ± 0.03) to 20 mm (0.04 ± 0.02) endoscope penetration depth.

There was a statistically significant difference in the share of the total field of view of MSF in the central opening at an endoscope viewing angle of 15° to endoscope penetration depth of 10 and 20 mm, respectively, $p \leq 0.05$, with SV of the total field of view of MSF decreasing from 10 (0.06 ± 0.02) to 20 mm (0.03 ± 0.02) endoscope penetration depth.

There was a statistically significant difference in the share of the total field of view of MSF in the distal opening at an endoscope viewing angle of 15° to endoscope penetration depth of 10 and 20 mm, respectively, $p \leq 0.05$, with SV of the total field of view of MSF decreasing from 10 (0.04 ± 0.02) to 20 mm (0.02 ± 0.01) endoscope penetration depth.

There was a statistically significant difference in the share of the total field of view of MSF in the medial opening at an endoscope viewing angle of 45° to endoscope penetration depth of 10 and 20 mm, respectively, $p \leq 0.05$, with SV of the total field of view of MSF decreasing from 10 (0.12 ± 0.02) to 20 mm (0.08 ± 0.02) endoscope penetration depth.

There was a statistically significant difference in the share of the total field of view of MSF in the central opening at an endoscope viewing angle of 45° to endoscope penetration depth of 10 and 20 mm, respectively, $p \leq 0.05$, with SV of the total field of view of MSF decreasing from 10 (0.12 ± 0.02) to 20 mm (0.07 ± 0.02) endoscope penetration depth.

There was a statistically significant difference in the share of the total field of view of MSF in the distal opening at an endoscope viewing angle of 45° to endoscope penetration depth of 10 and 20 mm, respectively, $p \leq 0.05$, with SV of the total field of view of MSF decreasing from 10 (0.12 ± 0.02) to 20 mm (0.07 ± 0.02) endoscope penetration depth.

SV of the total field of view of MSF to the 10 mm depth of penetration was constant for all three endoscopic access holes at a 45° endoscope viewing angle, whereas the share of the total field of view of MSF to the 20 mm depth of penetration decreased from medial (0.08 ± 0.02) to distal (0.07 ± 0.02).

There was a statistically significant difference in the share of the total field of view of MSF in the medial opening at an endoscope viewing angle of 90° to endoscope penetration depth of 10 and 20 mm, respectively, $p \leq 0.05$, with SV of the

total field of view of MSF decreasing from 10 (0.06 ± 0.02) to 20 mm (0.08 ± 0.02) endoscope penetration depth.

There was a statistically significant difference in the share of the total field of view of MSF in the central opening at an endoscope viewing angle of 90° to endoscope penetration depth of 10 and 20 mm, respectively, p≤0.05, with SV of the total field of view of MSF increasing from 10 (0.07 ± 0.02) to 20 mm (0.09 ± 0.02) endoscope penetration depth.

There was a statistically significant difference in the share of the total field of view of MSF in the distal opening at an endoscope viewing angle of 90° to endoscope penetration depth of 10 and 20 mm, respectively, p≤0.05, with SV of the total field of view of MSF increasing from 10 (0.08 ± 0.02) to 20 mm (0.10 ± 0.02) endoscope penetration depth.

Analysis of the data to the viewing angle with the endoscope

The analysed data for SV of the total field of view of the maxillary sinus to the viewing angle with the endoscope are shown in table 4.

There was a statistically significant difference in SV of the total field of view of MSF for medial opening and endoscope penetration depth of 10 mm to viewing angle of 15°, 45°, and 90°, respectively, p≤0.05, with the highest share of visibility observed at a viewing angle of 45° (0.12 ± 0.02) and the lowest share at 90° (0.06 ± 0.02).

There was a statistically significant difference in SV of the total field of view of MSF for medial opening and endoscope penetration depth of 20 mm to viewing angle of 15°, 45° and 90°, respectively - p≤0.05, with SV increasing from viewing angle of 15° (0.04 ± 0.02) to 90° (0.08 ± 0.02).

There was a statistically significant difference in SV of the total field of view of MSF for a central opening and 10 mm endoscope penetration depth to viewing angle of 15°, 45° and 90°, respectively, p≤0.05, with the highest share of visibility observed at an viewing angle of 45° (0.12 ± 0.02) and the lowest share at 15° (0.06 ± 0.02).

There was a statistically significant difference in SV of the total field of view of MSF for central opening and endoscope penetration depth of 20 mm to viewing angle of 15°, 45° and 90°, respectively p≤0.05, with SV increasing from viewing angle of 15° (0.03 ± 0.02) to 90° (0.09 ± 0.02).

There was a statistically significant difference in SV of the total field of view of MSF for distal opening and endoscope penetration depth of 10 mm to viewing angle of 15°, 45° and 90°, respectively p≤0.05, with the highest SV observed at viewing angle of 45° (0.12 ± 0.02) and the lowest share at 15° (0.04 ± 0.02).

There was a statistically significant difference of SV of the total field of view of MSF for distal opening and 20 mm endoscope penetration depth to viewing angle of 15°, 45° and 90°, respectively p≤0.05, with SV increasing from viewing angle of 15° (0.02 ± 0.01) to 90° (0.10 ± 0.02).

4. Discussion

There are not many reports in the literature focusing on dental implantology using endoscopically guided augmentation procedure to lift the MSF by using endoscopes with angled visual axis 0°, 30°, 45°, 70°, 90°, and 120° deviated from the instrument axis. The authors point to the endoscopically assisted MSF augmentation procedure as a minimally invasive technique with good visual control of the operative field, allowing detection of intraoperative Schneiderian membrane perforations during manipulation (1, 2, 4, 5, 7, 9). The literature describes the use of endoscopes with different angled visual axis in augmentation procedure of MSF lifting, but no studies were found to indicate the most optimal endoscopic approach with the highest SV of the total MSF area.

5. Conclusion

The same and highest SV of the total field of view of MSF was observed at all three endoscopic access openings (medial, central, distal) at 10 mm endoscope penetration and 45° viewing angle. The lowest SV of the total field of view of MSF was observed at the distal opening with an endoscope penetration of 20 mm and viewing angle of 15°.

References

[1] Berardini, Marco & Falco, Antonello & Amoroso, Cinzia & archivio, Lanfranco. (2015). Studio retrospettivo dei risultati clinici e radiologici di 69 rialzi di seno mascellare consecutivi associati a chirurgia endoscopica funzionale del seno (FESS). 10.11607/jomi.3757).
[2] Engelke W, Deckwer I. Endoscopically controlled sinus floor augmentation. A preliminary report. Clin Oral Implants Res. 1997 Dec;8(6):527-31.
[3] Engelke W., Beltran V., Endoscopic Techniques in Minimally Invasive Oral Surgery, Endo Press, 2014
[4] Gandhi Y. Endoscopically monitored maxillary sinus augmentation – Thechairside approach (Rationale and protocol). J Oral Biol Craniofac Res. 2020Jul-Sep;10(3):247-252. doi: 10.1016/j.jobcr.2020.05.002. Epub 2020 May 12.
[5] Hu YK, Yang C, Qian WT. Endoscopic-Assisted Sinus Floor Augmentation Combined With Removal of an Antral Pseudocyst of the Ipsilateral Maxillary Sinus. J Craniofac Surg. 2017 Sep;28(6):15491551.
[6] Köhler S.G.,Behrbohm H.,Thiele T.,Behrbohm W. THE SINUS LIFT: Practical Interdisciplinary Guide with a Description of the Berlin Training Model. Endo-Press, 2015
[7] Nkenke E, Schlegel A, Schultze-Mosgau S, Neukam FW, Wiltfang J. Theendoscopically controlled osteotome sinus floor elevation: a preliminaryprospective study. Int J Oral Maxillofac Implants. 2002 Jul-Aug;17(4):557-66.
[8] Sapundziev N., Endoscopy in otorinolaringology. Are there any borders?, MedInfo, 2021
[9] Wiltfang J, Schultze-Mosgau S, Merten HA, Kessler P, Ludwig A, Engelke W. Endoscopic and ultrasonographic evaluation of the maxillary sinus after

combined sinus floor augmentation and implant insertion. Oral Surg Oral Med Oral Pathol Oral Radiol Endod. 2000 Mar;89(3):288-91.

Application

Table 1

Opening	Penetration depth	Viewing angle	n observed region	Mean	SD	Max	Min	Range	Median	Q1	Q3	IQR
Medial	10 mm	45°	40	0,12	0,02	0,18	0,08	0,10	0,12	0,11	0,14	0,03
Central	10 mm	45°	40	0,12	0,02	0,18	0,07	0,10	0,11	0,10	0,13	0,03
Distal	10 mm	45°	40	0,12	0,02	0,16	0,08	0,08	0,11	0,10	0,13	0,03
Distal	20 mm	90°	40	0,10	0,02	0,14	0,05	0,10	0,10	0,08	0,11	0,03
Central	20 mm	90°	40	0,09	0,02	0,11	0,04	0,07	0,09	0,08	0,10	0,02
Medial	20 mm	45°	40	0,08	0,02	0,12	0,03	0,09	0,08	0,07	0,10	0,03
Medial	20 mm	90°	40	0,08	0,02	0,14	0,04	0,10	0,08	0,07	0,09	0,02
Distal	10 mm	90°	40	0,08	0,02	0,12	0,03	0,09	0,08	0,07	0,09	0,02
Central	20 mm	45°	40	0,07	0,02	0,11	0,03	0,08	0,07	0,06	0,09	0,03
Central	10 mm	90°	40	0,07	0,02	0,12	0,03	0,09	0,07	0,05	0,08	0,03
Distal	20 mm	45°	40	0,07	0,02	0,11	0,02	0,09	0,07	0,04	0,09	0,05
Medial	10 mm	15°	40	0,07	0,03	0,13	0,02	0,12	0,06	0,04	0,09	0,05
Medial	10 mm	90°	40	0,06	0,02	0,10	0,02	0,08	0,07	0,04	0,08	0,04
Central	10 mm	15°	40	0,06	0,02	0,11	0,01	0,10	0,05	0,04	0,07	0,03
Distal	10 mm	15°	40	0,04	0,02	0,09	0,01	0,08	0,04	0,03	0,05	0,02
Medial	20 mm	15°	31	0,04	0,02	0,08	0,01	0,08	0,04	0,02	0,05	0,03
Central	20 mm	15°	32	0,03	0,02	0,06	0,00	0,06	0,03	0,02	0,04	0,02
Distal	20 mm	15°	26	0,02	0,01	0,05	0,00	0,05	0,02	0,01	0,03	0,02

Table 2

Opening	Penetration depth	Viewing angle	n observed region	Mean	SD	Median	Q_1	Q_3	IQR	Range	Min	Max	F (ANOVA)	Kruskal Wallis	P
Medial	10 mm	15°	40	0,07	0,03	0,06	0,04	0,09	0,05	0,12	0,02	0,13		15,25	0,000
Central			40	0,06	0,02	0,05	0,04	0,07	0,03	0,10	0,01	0,11			
Distal			40	0,04	0,02	0,04	0,03	0,05	0,02	0,08	0,01	0,09			
Medial	20 mm	15°	31	0,04	0,02	0,04	0,02	0,05	0,03	0,08	0,01	0,08	6 327 080		0,00246
Central			32	0,03	0,02	0,03	0,02	0,04	0,02	0,06	0,00	0,06			
Distal			26	0,02	0,01	0,02	0,01	0,03	0,02	0,05	0,00	0,05			
Medial	10 mm	45°	40	0,12	0,02	0,12	0,11	0,14	0,03	0,10	0,08	0,18	1,974228		0,143468
Central			40	0,12	0,02	0,11	0,10	0,13	0,03	0,08	0,08	0,16			
Distal			40	0,12	0,02	0,11	0,10	0,13	0,03	0,10	0,07	0,18			
Medial	20 mm	45°	40	0,08	0,02	0,08	0,07	0,10	0,03	0,09	0,03	0,12	6,486057		0,002131
Central			40	0,07	0,02	0,07	0,06	0,09	0,03	0,08	0,03	0,11			
Distal			40	0,07	0,02	0,07	0,04	0,09	0,05	0,09	0,02	0,11			
Medial	10 mm	90°	40	0,06	0,02	0,07	0,04	0,08	0,04	0,08	0,02	0,10	6,606755		0,001912
Central			40	0,07	0,02	0,07	0,05	0,08	0,03	0,09	0,03	0,12			
Distal			40	0,08	0,02	0,08	0,07	0,09	0,02	0,09	0,03	0,12			
Medial	20 mm	90°	40	0,08	0,02	0,08	0,07	0,09	0,02	0,10	0,04	0,14		15,25	0,000
Central			40	0,09	0,02	0,09	0,08	0,10	0,02	0,07	0,04	0,11			
Distal			40	0,10	0,02	0,10	0,08	0,11	0,03	0,10	0,05	0,14			

Table 3

Penetration depth	Opening	Viewing angle	n observed region	Mean	SD	Median	Q_1	Q_3	IQR	Range	Min	Max	t test	Wilcoxon	P
10 mm	Medial	15°	40	0,07	0,03	0,06	0,04	0,09	0,05	0,12	0,02	0,13	10,374992		0,000
20 mm			31	0,04	0,02	0,04	0,02	0,05	0,03	0,08	0,01	0,08			
10 mm	Central	15°	40	0,06	0,02	0,05	0,04	0,07	0,03	0,10	0,01	0,11	9,326934		0,000
20 mm			32	0,03	0,02	0,03	0,02	0,04	0,02	0,06	0,00	0,06			
10 mm	Distal	15°	40	0,04	0,02	0,04	0,03	0,05	0,02	0,08	0,01	0,09		4,38	0,000
20 mm			26	0,02	0,01	0,02	0,01	0,03	0,02	0,05	0,00	0,05			
10 mm	Medial	45°	40	0,12	0,02	0,12	0,11	0,14	0,03	0,10	0,08	0,18	11,796176		0,000
20 mm			40	0,08	0,02	0,08	0,07	0,10	0,03	0,09	0,03	0,12			
10 mm	Central	45°	40	0,12	0,02	0,11	0,10	0,13	0,03	0,08	0,08	0,16	14,051088		0,000
20 mm			40	0,07	0,02	0,07	0,06	0,09	0,03	0,08	0,03	0,11			
10 mm	Distal	45°	40	0,12	0,02	0,11	0,10	0,13	0,03	0,10	0,07	0,18	12,458648		0,000
20 mm			40	0,07	0,02	0,07	0,04	0,09	0,05	0,09	0,02	0,11			
10 mm	Medial	90°	40	0,06	0,02	0,07	0,04	0,08	0,04	0,08	0,02	0,10		3,97	0,000
20 mm			40	0,08	0,02	0,08	0,07	0,09	0,02	0,10	0,04	0,14			
10 mm	Central	90°	40	0,07	0,02	0,07	0,05	0,08	0,03	0,09	0,03	0,12	5,97		0,000
20 mm			40	0,09	0,02	0,09	0,08	0,10	0,02	0,07	0,04	0,11			
10 mm	Distal	90°	40	0,08	0,02	0,08	0,07	0,09	0,02	0,09	0,03	0,12	4,87		0,000
20 mm			40	0,10	0,02	0,10	0,08	0,11	0,03	0,10	0,05	0,14			

Table 4

Viewing angle	Opening	Penetration depth	n observed region	Mean	SD	Median	Q_1	Q_3	IQR	Range	Min	Max	F (ANOVA)	Fridman	P
15°	Medial	10 mm	40	0,07	0,03	0,06	0,04	0,09	0,05	0,12	0,02	0,13			
45°			40	0,12	0,02	0,12	0,11	0,14	0,03	0,10	0,08	0,18			
90°			40	0,06	0,02	0,07	0,04	0,08	0,04	0,08	0,02	0,10	80,547022		0,000
15°	Medial	20 mm	31	0,04	0,02	0,04	0,02	0,05	0,03	0,08	0,01	0,08			
45°			40	0,08	0,02	0,08	0,07	0,10	0,03	0,09	0,03	0,12			
90°			40	0,08	0,02	0,08	0,07	0,09	0,02	0,10	0,04	0,14		42	0,000
15°	Central	10 mm	40	0,06	0,02	0,05	0,04	0,07	0,03	0,10	0,01	0,11			
45°			40	0,12	0,02	0,11	0,10	0,13	0,03	0,08	0,08	0,16			
90°			40	0,07	0,02	0,07	0,05	0,08	0,03	0,09	0,03	0,12	83,445118		0,000
15°	Central	20 mm	32	0,03	0,02	0,03	0,02	0,04	0,02	0,06	0,00	0,06			
45°			40	0,07	0,02	0,07	0,06	0,09	0,03	0,08	0,03	0,11			
90°			40	0,09	0,02	0,09	0,08	0,10	0,02	0,07	0,04	0,11	131,67423		0,000
15°	Distal	10 mm	40	0,04	0,02	0,04	0,03	0,05	0,02	0,08	0,01	0,09			
45°			40	0,12	0,02	0,11	0,10	0,13	0,03	0,10	0,07	0,18			
90°			40	0,08	0,02	0,08	0,07	0,09	0,02	0,09	0,03	0,12		60	0,000
15°	Distal	20 mm	26	0,02	0,01	0,02	0,01	0,03	0,02	0,05	0,00	0,05			
45°			40	0,07	0,02	0,07	0,04	0,09	0,05	0,09	0,02	0,11			
90°			40	0,10	0,02	0,10	0,08	0,11	0,03	0,10	0,05	0,14	166,75878		0,000

Author Profile

Desislava Kirilova Stoyanova, Assistant Professor at Department of Periodontology and Dental Implantology, Medical University of Varna, Bulgaria,dr.dess.stoyanova@gmail.com

Stefan Vasilev Peev, DMD, PhD, DSc, Professor (Full) at Department of Periodontology and Dental Implantology, Medical University of Varna, Bulgaria, stefan.peev@mail.bg

Nikolay Rumenov Sapundziev, DMD, Professor (Associate) at Department of Neurosurgeryand Otorhinolaryngology, Medical University of Varna, Bulgaria, n.sapundziev@gmail.com

Anjela Ivanovna Bakhova, Assistant Professor at Faculty of Public Health, Medical University of Varna. bakhova@gmail.com